Exploring the medicinal potential of in vitro cultures for enhanced production of metabolite empowered by green silver nanoparticles in Alhagi maurorum Medik

DEEPAK BAMAL
Maharshi Dayanand University Rohtak
ANITA RANI SEHRAWAT
anitasehrawat@mdurohtak.ac.in
Maharshi Dayanand University Rohtak https://orcid.org/0000-0003-0594-1929
ANOOP SINGH
Maharshi Dayanand University Rohtak
NISHA SWAMI
Maharshi Dayanand University Rohtak

Research Article

Keywords: Alhagi maurorum, Tissue culture, Silver nanoparticles, antioxidants, Secondary metabolites

Posted Date: November 10th, 2023

DOI: https://doi.org/10.21203/rs.3.rs-3500246/v1

Abstract

Alhagi maurorum, a valuable medicinal plant, presents an opportunity for sustainable biomass production and the amplification of therapeutic compounds. Here, MS Medium containing BAP (3.0 mg/L), NAA (0.1 mg/L), kinetin (0.50 mg/L) and including ascorbic acid (50.0 mg/L), adenine sulfate (25.0 mg/L), citric acid (25.0 mg/L), and arginine (25.0 mg/L) were used for callus formation, multiplication and differentiation from shoot tip with cotyledons and hypocotyl explants. The effectiveness of biologically synthesized silver nanoparticles (AgNPs) on the growth, differentiation of calli, plantlet formation and antioxidant accumulation of *Alhagi maurorum* tissues was investigated. The biogenic AgNPs synthesis and characterization were confirmed UV-Vis spectroscopy. The size shape and nature were confirmed via zeta potential, FTIR, XRD, SEM, and TEM analysis. Incorporating green-synthesized AgNPs (2.0, 4.0, 6.0, 8.0, 10.0, and 12.0 mg/L) in conjunction with plant growth regulators, significantly promoted embryogenic callus formation, proliferation and differentiation, demonstrating nanotechnology's potential in plant tissue culture. Adding 8.0 mg/L AgNPs in callus cultures showed higher accumulation of total soluble protein (45.56 and 43.58 mg/gDW), total free amino acids (17.46 and 16.56 mg/gDW), and total starch (43.59 and 32.43 mg/gDW) from cotyledons and hypocotyl, respectively. Total phenolic compounds (185.68 and 179.40 mg/g DW GAE), total flavonoids (71.38 and 68.01 mg/gQE) from cotyledons and hypocotyls, respectively were reported in the cultures raised at 8.0 mg/L AgNPs concentration in MS media. Enhanced activities of superoxide dismutase (97.83 and 93.34% inhibition), peroxidase (2.54 and 2.42 U), catalase (65.63 and 65.50 U), ascorbate peroxidase (0.61 and 0.49 mM/mg FW), and glutathione reductase (0.96 and 0.78 U), were reported at the same concentration of AgNPs for cotyledon and hypocotyl derived tissues, respectively. Future research should focus on elucidating the molecular mechanisms governing nanoparticle-plant interactions and addressing potential health challenges. Hence, the present research shed light on the therapeutic significance of *Alhagi maurorum* and the potential applications of AgNPs in the enhanced production of valuable compounds.

1. Introduction

Plants have long been recognized for their remarkable medicinal and nutritional properties, owing to the presence of bioactive compounds. Traditional medicine remains a primary source of healthcare for the global population, emphasizing the ongoing relevance of plant-based remedies (Vaou et al. 2021). Among the countries, known for their rich herbal heritage, India stands out a significant producer of medicinal plants and herb products, with well-established traditional systems of medicine such as Naturopathy, Homeopathy, Ayurveda, Siddha, and Unani (Samal, 2016).

Alhagi maurorum, commonly called camelthorn (Family Fabaceae) has gained attention due to its extensive medicinal applications. This green, thorny, perennial shrub often growing up to 1.0 meter tall. It thrives in dry lands with low rainfall, and its roots can penetrate as deep as 5–7 meters, making it resilient in harsh environments characterized by high salinity and alkalinity (King, 1974). Traditionally, *Alhagi maurorum* has been employed to remedy various conditions, including rheumatic pains, gastrointestinal discomfort, urinary tract, and liver diseases. Its versatile properties include diaphoretic, diuretic, expectorant, analgesic, antipyretic, anti-inflammatory, and laxative effects, while its efficacy in treating ulcers has been extensively reported (Khalifa 2019; Kulieva et al. 1972; Ahmed et al. 2009). Notably, the active fraction lupeol, detected in *Alhagi maurorum* through nuclear magnetic resonance, has shown the potential to induce apoptosis in human breast cancer cells (Bahamin et al. 2021).

However, *Alhagi maurorum* has significantly declined due to habitat destruction, chemical-intensive agricultural practices, poor seed germination, limited attractiveness, and insufficient awareness of its medicinal value. As a result, preserving and utilizing this plant for medicinal purposes has become imperative. In recent years, plant tissue culture systems have emerged as a promising avenue for producing valuable therapeutic compounds that are otherwise challenging to obtain naturally. These systems offer a renewable source of such compounds through controlled and sustainable cultivation. However, addressing microbial contamination remains a significant challenge in plant tissue culture. Despite various disinfection methods and agents employed to combat pathogens, resistance often emerges, leading to recurring contamination outbreaks (Sehrawat et al. 2021).

Nanoparticles, particularly metal nanoparticles, have gained attention as potent elicitors of plant secondary metabolism. Their unique properties, including enhanced reactivity, physical characteristics, and potential applications in diagnostics, drug delivery, and antimicrobial studies, make them promising candidates for stimulating secondary metabolite production (Amer et al. 2019; Bamal et al. 2021). Silver nanoparticles (AgNPs) have demonstrated extensive use in various fields, including antimicrobial applications, orthopedics, drug delivery systems, and diagnostics (Bruna et al. 2021). Their catalytic activity, thermal and optical properties, and broad-spectrum antimicrobial effects contribute to their significance. This research article aims to explore the medicinal potential of *Alhagi maurorum* comprehensively. It investigates the plant's primary and secondary metabolite profiles, focusing on the influence of AgNPs on secondary metabolite accumulation.

2. Material and Methodology

2.1 Seed Germination

Seeds of *Alhagi maurorum* were collected in the month of October from ripe pods in Rohtak, Haryana (28°54'23.8"N 76°37'00.3"E). After de-husking, the seeds were pre-soaked in hot water. Sterilization was done with 0.1% $HgCl_2$, (4.0 min.). Seeds were washed (3–4 times) and then placed on germination medium (autoclaved at 121°C for 20 minutes) containing 3.0% sucrose and 0.8% agar. Ten days-old seedling explants (shoot tip with cotyledon and hypocotyl) were used for further studies.

2.2 Establishment of Cultures

A ready-made MS (Murashige and Skoog's, 1962) medium supplemented with B5 vitamins and sucrose was acquired from Hi-Media. The growth regulators, BAP (3.0 mg/L), NAA (0.1 mg/L), and kinetin (0.50 mg/L), were added. Additional compounds, including ascorbic acid (50.0 mg/L), adenine sulfate (25.0 mg/L), citric acid (25.0 mg/L), and arginine (25.0 mg/L) were also added, Biogenic silver nanoparticles (AgNPs 2.0, 4.0, 6.0, 8.0, 10.0, and 12.0 mg/L) were added and the medium was autoclaved at a temperature of 121°C at 15 psi for 20 minutes. The control medium was without AgNPs, Shoot tip with cotyledon (C) and hypocotyl (H) explants from 10-days-old seedlings were inoculated on MS Medium with different composition of green silver nanoparticles and on control medium. The observations for day-to-callus induction, percent response, differentiation, and effects of green silver nanoparticles on callus as well as phytoconstituents accumulation were recorded.

2.3 Synthesis of Green Silver Nanoparticles

The Fresh leaves (10.0 g) were washed and crushed, in distilled water. Their aqueous extract was prepared by adding 100.0 ml of distilled water. Ten ml extract was used for the biogenic synthesis of silver nanoparticles by adding 0.1 mM silver nitrate solution with continuous stirring. The color change was observed from yellowish to dark brown. The AgNP solution was kept in the dark. The synthesized nanoparticles were purified via centrifugation. The characterization of AgNPs was done by UV-Vis spectroscopy, Zeta Potential study, Fourier Transform Infrared Spectroscopy (FTIR) spectroscopy, X-ray Diffraction (XRD), Scanning Electron Microscopy (SEM), and Transmission Electron microscopy (TEM) studies.

2.4 Characterization of AgNPs

2.4.1 UV-Vis Spectroscopy

Silver nitrate reduction was monitored via UV-Vis spectroscopy to identify the absorbance peak at a range from 300–700 nm. The stability was evaluated at multiple time intervals, from minutes to 60 days. (Cao et al. 2011; Chapman et al. 2011 and Rajeshkumar et al. 2017; Devi et al. 2013; McDonald et al. 2001).

2.4.2 Zeta Potential analysis

Zeta potential and nanoparticle size are critical factors influencing both stability and toxicity, Zeta potential affects adsorption onto cell membranes and particle size determining endocytosis uptake. Synthesized AgNPs after 24 hours of incubation, were purified by centrifugation, and dispersed in sterile distilled water to remove uncoordinated biological molecules. The purified pellets were then oven-dried at 60°C for 2 hours. Then, AgNP suspension was sonicated for 20 minutes for zeta potential analysis.

2.4.3 Fourier Transform Infrared (FTIR) Spectroscopy

The chemical composition of synthesized silver nanoparticles (AgNPs) was ascertained using Fourier Transform Infrared (FTIR) Spectroscopy. FTIR spectroscopy was employed to identify functional and stability-related groups which were associated with biomolecules of plant extract and responsible for the reduction of Ag°. These essential functional groups were identified within the 400–4000 cm^{-1} wave number range. (Kainat et al. 2022)

2.4.4 X-ray Diffraction (XRD) Study

X-ray Diffraction (XRD) technique used for assessing the particle sizes, crystallinity, and isomorphous substitutions. It provides qualitative and quantitative resolution of chemical compounds by projecting the X-ray beam onto a crystal, generating diffraction patterns according to Bragg's law, and confirmed the crystalline nature of nanoparticles (Cao et al. 2011; Chapman et al. 2011 and Rajeshkumar et al. 2017). Green-synthesized, centrifuged, oven-dried, purified, powdered pellets were used for X-ray diffraction (XRD) analysis to investigate the crystal structure.

2.4.5 Scanning Electron Microscopy (SEM) Study

Scanning Electron Microscopy (SEM), an imaging tool used to analyze the nanomaterial particle size, distributions, shapes, and surface morphology at the nanoscale. SEM is applicable to solid powdered and liquid samples. After 24 hours of incubation, green-synthesized AgNPs were purified dispersed in sterile distilled water to eliminate uncoordinated biological molecules. The purified pellets were then oven-dried at 60°C for 2 hours. Then, for SEM analysis, powdered and sonicated AgNPs suspension was applied to carbon-coated copper SEM grids for examination and imaging (Devi et al. 2013).

2.4.6 Transmission Electron microscopy (TEM) assessment

Transmission Electron microscopy (TEM) assesses the size and shape of synthesized nanoparticles. After 24 hours of incubation, dried purified pellets were dissolve in water, sonicated (20 min.) and used for TEM analysis. The sonicated suspension was placed on carbon-coated copper TEM grids and allowed to dry, and used observations (McDonald et al. 2001).

2.5 Primary Metabolites quantification

Field plant parts, air-dried calli and regenerated tissues were used to quantify starch, soluble sugars, total proteins, and free amino acids. The respective established protocols with minor modifications were used for their quantification by Dubois' (1956); Anthrone (1962); Bradford (1976); Sadasivam and Manickam's (1992) methods. Dried tissues were homogenized in 80% ethanol. The mixtures were heated at 60℃ for 20 min., then centrifuged at 5000 rpm for 15 min. The supernatant was collected and concentrated to one-fifth of its original volume. The prepared supernatant was stored at 4℃ for further use.

2.5.1 Quantification of Soluble Sugar

Soluble sugar content in each extract was quantified using Duboi's (1956) method. One ml of 80% phenol was added to 0.1 ml sample, after gentle agitation, 5.0 ml concentrated sulfuric acid was added, and then, subsequent incubation was done. The absorbance at 420 nm of the resulting color complex was done. The quantification of soluble sugars was done using glucose as standard.

2.5.2 Estimation of Starch Content

Starch content in filtration residue was done by Anthrone (1962) method. 10.0 ml of 1% HCl was added to the residue of primary metabolites centrifuged extract and kept in the water bath for 30 min at 100 C. After centrifugation supernatant was collected. 1 ml of ice-cold Anthrone Reagent was added into 1.0 ml of extract & incubate for 10 min. at room temperature. A change in the color intensity was observed at 649 nm. Estimation of Starch in each sample was done by plotting standard curve of starch.

2.5.3. Assessment of Total Soluble Protein

The soluble protein in all the samples was assessed using the Bradford (1976) method. Each sample (0.5 ml) was mixed with 1.0 ml Bradford reagent and incubated for 10 minutes at room temperature. The absorbance for calculating total protein content was determined at 595 nm. The standard curve constructed with bovine serum albumin was used as a standard for quantification of soluble proteins in each sample.

2.5.4 Evaluation of Total Free Amino Acids

Sadasivam and Manickam's (1992) protocol was employed to measure total free amino acids in all samples. A mixture of ninhydrin (1.0 ml), plant extract (0.1) ml and distilled water (0.9 ml) was prepared and after total volume of 2.0 ml, samples were heated for 20 min., 5.0 ml diluent (2.5 ml distilled water + 2.5 ml n-Propanol) was added and incubated for 15 min. The purple complex was obtained. Absorbance at 570 nm was recorded for amino acid determination. The amino acid content in each sample was quantified using leucine as a standard by plotting estimation curve.

2.6 Non-Enzymatic Assays

2.6.1 Plant Extract Preparation for Antioxidants Assays

Air-dried samples (10.0 g) were homogenized in 80% methanol and 100 ml total volume was prepared. The samples were heated at 60ºC for 20 min. After 24 hours of agitation, centrifugation was done at 5000 rpm for 15 min. The collected supernatant was evaporation and reduced to one-fifth of its original volume. Samples were stored at 4ºC for further experiments.

2.6.1.1 Free Radical Scavenging Activity via DPPH assay

Bloi's (1958) protocol was used for free radical scavenging activity. Plant extract (0.1 ml) was mixed with 2.0 ml of 0.3 mM DPPH (prepared in 80% methanol). The samples were serially diluted and incubated for 30 min. at room temperature. Free radical scavenging activity

assays assessed by measuring absorbance at 517 nm. The quantification was done by using following formula:

$$\%\mathbf{scavengingactivity} = \frac{\mathbf{Acontrol - Asample}}{\mathbf{Acontrol}} \text{ X } 100$$

A- Absorbance

2.6.1.2 Assessment of Total Phenolic Content

The Folin-Ciocalteu method was used to assess the total phenolic content (Singleton et al. 1999). Each sample (0.1 ml) at 100 µg/ml concentration was mixed with 0.1 ml Folin-Ciocalteu reagent and incubated for 15 minutes. Then, after 30 min., 20% Na_2CO_3 (2.5 ml) solution was added and absorbance at 760 nm was determined. The phenols in each sample was calculated against a gallic acid standard curve.

2.6.1.3 Estimation of Total Flavonoids Content

The total flavonoid content in samples were determined using the method of Hertog et al. (1993). Aluminum chloride solution (1.0%) prepared in 80% methanol. Each 0.1 ml sample (100 µg/ml) was mixed with 1.5 ml aluminum chloride solution, followed by a 10 min. dark incubation. Absorbance of each sample was measured at 415 nm. The flavonoids quantification was done by plotting quercetin standard curve at different concentrations.

2.6.2. Sample preparation for Enzymatic Assays

Haida and Hakiman (2019) method was followed for the preparation materials. Experimental material (10.0 g) was homogenized in 100.0 ml of 0.1M potassium phosphate buffer (pH 7.0) containing 800 mg polyvinyl pyrrolidone (PVP). The samples were centrifuged at 10,000 rpm for 30 min. and supernatants were collected for enzymatic assays.

2.6.2.1 Superoxide Dismutase (SOD) Assay

Superoxide Dismutase (SOD) activity assays was done by Misra and Fridovich, (1972) method. Reaction mixture with 0.5 ml of each 0.1 mM EDTA, 13.0 mM methionine, 2.0 µM riboflavin, 75.0 µM Nitrobluetetrazolium chloride (NBT) was taken, and then, 0.1 ml sample was added. Following a 10 min. incubation at room temperature in dark, SOD activity was measured at 560 nm. The activity was calculated with one unit as the amount of enzyme that inhibits 50% of NBT reduction.

$$\text{\% Inhibition} = \frac{\mathbf{Acontrol - Asample}}{\mathbf{Acontrol}} \text{X } 100$$

A- Absorbance

2.6.2.2 Peroxidase Activity Assay

Peroxidase activity was determined using the guaiacol oxidation method of Chance and Maehly (1955). Four ml reaction mixture contained 2.9 ml of 0.1 mM H_2O_2 prepared in 0.1 M sodium phosphate buffer (pH 7.0), 1.0 ml of 0.3 mM guaiacol (prepared in ethanol), and 0.l ml of enzyme extract. The increase in absorbance was recorded at 436 nm against the control. The unit of peroxidase activity was expressed as the amount of enzyme required to decompose 1.0 µmol of H_2O_2 per minute at 25°C and pH 7.0. A standard curve of H_2O_2 (µ moles) has been plotted to calculate the activity units of peroxidase.

2.6.2.3 Catalase Activity Assay

Catalase activity was determined by measuring a decrease in the absorbance at 240 nm due to the decomposition of H_2O_2 by the enzyme (Aebi et al. 1984). The reaction was initiated by adding 0.1 ml enzyme extract to 2.9 ml of reaction mixture containing 3.0 mM H_2O_2 prepared in 0.01 M sodium phosphate buffer (pH 7.0). A decrease in absorbance at 240 nm for 3 min was recorded against the control. One unit of enzyme activity is defined as the amount of enzyme required to decompose 1.0 µmol of H_2O_2 per minute at 25°C and pH 7.0. Catalase activity was calculated using the extinction coefficient of 39.4 mM^{-1} cm^{-1} in the given formula:

$$\mathbf{Catalase\,(UnitActivity)} = \frac{(\varvec{\Delta}\mathbf{AChangeinabsorbance}) \times \mathbf{VolumeofTotalSample}}{\varvec{\Delta}\mathbf{tXExtinctionCoefficient\,(\text{l})\,XDiameterofCuvette\,(l)\,Xvolofenzyme}}$$

2.6.2.4 Ascorbate Peroxidase Activity

The method of Asada (1992) was followed for measuring ascorbate peroxidase activity. The reaction mixture contained an equal volume (0.4 ml) of 0.5 mM ascorbate, 0.1 mM hydrogen peroxide, 0.1 mM EDTA, 0.1 ml of enzyme extract, and 1.7 ml of 0.01M potassium phosphate buffer (pH 7.0) to make a final volume of 3.0 ml. A decrease in absorbance was recorded at 290 nm immediately after every 1 min up to 10 min. One unit of enzyme activity was defined as the amount of enzyme required to decompose ascorbate per minute at 25°C and pH 7.0. Ascorbate activity was calculated using the extinction-coefficient of 2.8 mM^{-1} cm^{-1} in the given formula:

$$\mathbf{Ascorbate\,(UnitActivity)} = \frac{(\varvec{\Delta}\mathbf{AChangeinabsorbance}) \times \mathbf{VolumeofTotalSample}}{\varvec{\Delta}\mathbf{tXExtinctionCoefficient}\,(\square)\,\mathbf{XDiameterofCuvette}\,(\mathrm{l})\,\mathbf{Xvolofenzyme}}$$

2.6.2.5 Glutathione Reductase activity

The glutathione reductase activity was assayed spectrophotometrically by Smith et al. 1988. In the reaction mixture, equal volumes (0.5 ml) of 0.1 mM EDTA, 0.01M potassium phosphate buffer (pH 7.0), 3 mM DTNB (5,5ç-Dithiobis (2-nitrobenzoic acid), 2 mM oxidized glutathione (GSSG) and 2 mM NADPH (β-nicotinamide adenine dinucleotide phosphate, reduced) were mixed. 0.1 ml of enzyme extract was mixed, and absorbance at 412 nm was measured. One unit will cause the reduction of 1.0 µmole of DTNB to TNB at 25°C and pH 7.5. A standard curve of H_2O_2 (µ moles) has been plotted to calculate the activity units of peroxidase.

2.7 High Performance Liquid Chromatography (HPLC) profiling

The extract was prepared using dried samples (0.1g) in 10.0 ml of 80% ethanol. The samples were kept at shaker incubator for 48 hours at 150 rpm. After centrifugation, filtration was done through a 0.22µm PTFE syringe. About 10.0 µl of the filtered extract was injected into the column for analysis. A reference standard, Lupeol was prepared and used for calibration purposes (Khalid et al. 2023). HPLC analyses utilized a waters liquid chromatograph system with a model 600 solvent pump and a 2996 photodiode array detector (Waters, Milford, MA, USA). Data acquisition employed Vest v.2 Software. Chromatography utilized a C18 reversed-phase column (Lichro Sorb RP18, 4.6×150 mm, 5 µm, Merck, Darmstadt, Germany).

3 Result and Discussion

3.1 Seed germination and establishment of cultures

The choice of explants and their ability to regenerate at high frequency is important for tissue culture studies. *In-vitro* raised seedling was used as a source of explants for culture establishment (Fig. 1). The seeds showed very poor germination (Fig. 1b), and we achieved 63.0% germination (Fig. 1c), when the seed was soaked in hot water for ten minutes. The soaked seeds were sterilized in 0.1% $HgCl_2$ for 4 min.

Shoot tip with cotyledons and Hypocotyls (1.0–1.5 cm) from i*n-vitro* raised seedlings were inoculated on MS medium (Fig. 2a and b) augmented with B5 vitamins, growth regulators like BAP (3.0 mg/L), NAA (0.1 mg/L, and kinetin (0.50 mg/L). Other adjuvants, ascorbic acid (50.0 mg/L), adenine sulfate (25.0 mg/L), citric acid (25.0 mg/L), arginine (25.0 mg/L) were also added in the control medium. One week was required to initiate calli formation. Good calli was observed from hypocotyl (82%, Fig. 3) and shoot tip with cotyledon explants (100% Fig. 4) at four week.

3.2 Biosynthesis and Characterization of AgNPs

The AgNPs were biologically synthesized using the aqueous extract of *Alhagi maurorum*. Synthesis of silver nanoparticles was initially visualized by a change in the color of the reaction mixture from whitish yellow to dark brown (Fig. 6a). The reaction mixture developed a dark radish brown color very quickly, emphasizing the role of various biomolecules in green synthesis of nanoparticles as the control silver nitrate solutions (without leaf extract) neither developed the brown color nor did they display the characteristic peaks. Biocompatible and stable silver nanoparticles were thus synthesized after one hr. Further, the effect of time interval on the synthesis and the stability of silver nanoparticles was studied and it was observed that these AGNPs were remained stable up to two months (Fig. 6b)

Biogenic AgNPs were characterized using UV-visible spectrophotometer, Zeta potential, FTIR XRD, SEM, & TEM. The formed AgNPs were initially characterized by a UV-visible spectrophotometer at 300–700 nm optical spectrum. A peak at 421 nm confirmed the synthesis of green AgNPs. (Fig. 7a). The stability of the colloidal solution was evaluated via zeta potential analysis, which measures the surface charge of the fabricated nanoparticles. The recorded zeta potential value was − 18.8 mV ± 4.30 mV (Fig. 7b), signifying that the nanoparticles possessed a negative charge and displayed a notably high level of stability. To ensure nanosuspension stability, a minimum zeta potential of ± 30 mV is typically required (Ubgade et al. 2021). The negative zeta potential in silver nanoparticles, likely due to bio-organic capping from plant extracts, enables electrostatic repulsion, preventing agglomeration and ensuring stability (Liaqat et al. 2022).

Functional groups in the AgNPs colloidal solution were analyzed via Fourier-transform infrared spectroscopy (FTIR) in the 400–4000 cm^{-1} wavenumber range. The peaks exhibited at 2915, 2847, 1575, 1488, 1301, 1062, 810, and 702 cm^{-1} in the AgNPs solution (Fig. 8a). These peaks represent O-H stretching (2915, 2847, strong), C = N stretching (1575), C-O stretching (1301, 1062), C = C stretching (810, 702, weak), and vibrations, respectively. The X-Ray Diffraction (XRD) pattern of the synthesized AgNPs displayed strong and sharp peaks at (2θ) 27.92°, 32.34°, 46.32° 54.88° corresponds to (111), (200), (220), and (311) planes, respectively (JCPDS File No.: 01-1167) with the majority of particles showing (111) plane having face-centered cubic structure (Fig. 8b). SEM analysis confirmed that silver nanoparticles can be irregular, spherical, or round shape. Clusters have appeared in very large numbers. On average, AgNP size was between 7 to 40 nm (Fig. 9a and b). TEM analysis revealed AgNPs with spherical morphology, exhibiting sizes ranging from 7.45 to 30.7 nm (Fig. 9c).

3.3 Effect of Biogenic AgNPs on growth and differentiation of calli

Swelling and initiation of shoot buds appeared after four weeks of culturing. Embryogenic calli of hypocotyls and shoot tip with cotyledons were subcultured MS medium with different concentration of green synthesized AgNPs (2.0, 4.0, 6.0, 8.0, 10.0 and 12.0 mg/L). The control MS medium was without AgNPs. All the tested concentrations of green AgNPs showed its effect and a good growth of calli was observed but, MS Medium supplemented with 6.0 mg/L and 8.0 mg/L AgNPs were showed better response in term of multiple shoots with shoot buds and differentiation from both hypocotyls (Fig. 10) and cotyledons with shoot tip derived calli (Fig. 11). Cotyledons with shoot tip derived calli behaved better for multiple shoot formation as compared to hypocotyl calli. (Fig. 12). Auxins and cytokinins are well-known hormones used to obtain callogenesis or organogenesis, acting in synergy (Malabadi et al. 2012). Our results match with the study of Hassanein and Mazen (2001), where they studied adventitious bud formation in *Alhagi graecorum.* Explants are primarily oriented to organogenesis when auxins and cytokinins are used in combinations. Comparable findings were mentioned by Aggarwal et al. (2015) by culturing nodal segments of *Alhagi maurorum* on MS medium with 2.0 mg/L BAP. Zia et al. (2020) explored the influence of AgNPs on root and shoot development in different cultivars (*Noblessa*, *Antigua*, and *Mariposa*), revealing enhanced shoot production at lower concentrations (6.0 mg/L) and increased root number and length at 12.0 mg/L.

AgNPs in MS medium significantly improved shoot regeneration and plant survival in *Tecomella undulata*, an endangered medicinal plant, by inhibiting ethylene signaling (Aghdaei et al. 2012). In Khan et al. (2023) studied that Urea-doped silver nanoparticles (U-AgNPs) at 3.0 and 6.0 mg/L concentrations enhanced root and shoot growth in seedlings, with the most substantial effects observed at 6.0 mg/L. Moreover, U-AgNPs positively influenced root length starting from 1.5 mg/L and significantly increased fresh and dry weights at 6.0 mg/L. The study also demonstrated that *Alunus nitida*-AgNPs and Urea-Doped AgNPs at 3.0 and 6.0 µg/ml, respectively, promoted greater fresh and dry weights in wheat seedlings but negatively impacted shoot length at 15.0 µg/L, indicating potential toxicity at higher concentrations.

3.4 Effect of AgNPs on Primary Metabolite

The present research quantified metabolites like starch, soluble sugars, proteins, and free amino acids and assessed their modulation in response to AgNPs.

3.4.1 Total Soluble Sugar Accumulation

This study evaluated the soluble sugar content of various tissues *(in vitro and in vivo*) to determine its role in combating abiotic stresses. The treatments having 6.0 mg/L AgNPs showed the highest soluble sugar levels in cotyledons with shoot tip (174.45 ± 0.19 mg/gDW) as well as when hypocotyl (160.80 ± 0.31 mg/gDW) were cultured. On the other hand, at 12.0 mg/L both cotyledons with shoot tip and hypocotyl cultures showed the lowest sugar content, 137.73 ± 0.29 mg/gDW and 110.48 ± 0.25 mg/gDW, respectively The sugar content in field-grown leaves, shoots, and roots varied, shoots having the highest levels (151.95 ± 0.11 mg/gDW). The AgNPs (8.0 mg/L) resulted in substantially increased sugar content in regenerated shoots (178.583 ± 0.29 mg/gDW) compared to controls, while regenerated roots showed a modest response to the same treatment (67.21 ± 0.22 mg/gDW) (Fig. 13a). These findings demonstrate the potential of AgNPs in modulating soluble sugar levels in different plant tissues, which could have significant implications for stress tolerance and regeneration strategies. According to this research, using AgNPs led to a rise in soluble sugar levels within plant tissues, with callus cultures and regenerated shoots demonstrating the most significant increase. Regenerated shoots had the highest sugar concentration, with the treatment having 8.0 mg/L of AgNPs which had the most considerable impact on sugar content. These findings hold the potential for enhancing plant stress tolerance and regeneration techniques. Shaikhaldein et al. (2022) revealed that AgNPs (0, 10.0, 20.0, and 30.0 mg/L) to *Maerua oblongifolia* shoots significantly alleviates the adverse effects of salt stress and ameliorates plant developmental-related parameters and defense systems. High salinity elevates the oxidative damage by over-accumulation of the levels of total soluble sugars.

3.4.2 Estimation of total Soluble Protein Content

Proteins, central to cellular metabolism, were quantified using the Bradford (1976), method. Notably, AgNPs (8.0 mg/L) displayed the highest total soluble protein content when shoot tip with cotyledons (45.56 ± 0.07 mg/gDW) and hypocotyl (43.58 ± 0.07 mg/gDW) cultures

were evaluated while AgNPs (12.0 mg/L) showed the lowest protein in shoot tip with cotyledons (33.42 ± 0.06 mg/gDW) and hypocotyl (33.12 ± 0.06 mg/gDW). Field-grown leaves, shoots, and roots exhibited distinct protein levels (35.54 ± 0.16 mg/gDW, 30.38 ± 0.07 mg/gDW, and 15.34 ± 0.06 mg/gDW, respectively). It was observed that regenerated shoots, had 28.313 ± 0.088 mg/gDW protein accumulation which was lower in AgNPs (8.0 mg/L) treated culture where 42.27 ± 0.096 mg/gDW total soluble protein content was noticed. Regenerated roots of control culture accumulated 13.3 ± 0.03 mg/gDW and AgNPs (8.0mg/L) treated culture had 18.23 ± 0.07 mg/gDW total soluble protein content (Fig. 13b). Low AgNP concentrations (6.0 mg/g AgNPs) increased plant protein content in *phaseolus vulgaris* and *Zea mays*, while high concentrations (100 ppm AgNPs) decreased it, possibly due to AgNPs toxicity (Salama et al. 2012; Liu X., 2005). Variations were observed among AgNPs-treated plants of *Maerua oblongifolia*, with the lower concentration (10.0 mg/L) resulting in the high protein levels and higher concentrations (40.0 and 50.0 mg/L) causing reduced protein content accumulation (Shaikhaldein et al. 2020). These changes may be attributed to oxidative stress-induced protein modifications (Sharma et al. 2012).

3.4.3 Total Free Amino Acid Content

Total free amino acids serve as precursors to aromatic compounds in plants and play a pivotal role in cell growth. AgNPs (8.0 mg/L) on shoot tip with cotyledons and hypocotyl raised cultures exhibited the accretion of highest total free amino acids (17.46 ± 0.167 mg/gDW and 16.56 ± 0.107 mg/gDW, respectively), while the lowest piles of amino acids were found in AgNPs with 2.0 mg/L concentration with both the cultures (13.47 ± 0.043 mg/gDW, 11.43 ± 0.053 mg/gDW). Leaves, shoots, and roots from the field-grown plants gathered 9.12 ± 0.04 mg/gDW, 8.17 ± 0.04 mg/gDW, and 4.48 ± 0.208 mg/gDW, respectively of total free amino acids. When regenerated shoots of control was compared with AgNPs (8.0mg/L) it was noticed that total free amino acid content store was 8.30 ± 0.044 mg/gDW and 12.62 ± 0.091 mg/gDW, respectively, and a similar pattern of aggregation was observed in regenerated roots of control culture (4.14 ± 0.07 mg/gDW) and AgNPs (8.0 mg/L) treated culture (5.86 ± 0.059 mg/gDW, Fig. 13c). Mehrian et al. (2015) defined that in *Lycopersicon esculentum* free amino acid content increased significantly up to 100 mg/L AgNPs concentrations, and after that, declined significantly. Free amino acids are potential metal ligands and their increase under AgNPs stress is a strategy to modulate AgNPs effects. Azooz et al. (2012) suggested that the increase in total free amino acids under Cu^{2+} stress might be a detoxification response of wheat (*Triticum aestivum* cv. Hasaawi) to toxic level of copper nanoparticles.

3.4.4 Total Starch Estimation

Starch is a major storage metabolite of plants, which is synthesized mainly in plastids and accumulated in storage organs and seeds of plants. The amount of starch was maximum at 8.0 mg/L of AgNPs from shoot tip with cotyledons (43.59 ± 0.24 mg/gDW) and hypocotyl (32.43 ± 0.16 mg/gDW) obtained cultures while minimum in (35.69 ± 0.16 mg/gDW, 24.43 ± 0.13 mg/gDW respectively when AgNPs concentration was 12.0 mg/L. Field-grown leaves, shoot, and root had starch content of 41.41 ± 0.09 mg/gDW, 37.28 ± 0.09 mg/gDW, and 13.30 ± 0.09 mg/gDW, respectively. Starch clutter in regenerated shoots, root of control and 8.0 mg/L AgNP's treatment shoot, root had 35.24 ± 0.12 mg/gDW; 18.32 ± 0.07 mg/gDW and 45.42 ± 0.12; mg/gDW 21.267 ± 0.067 mg/gDW respectively. (Fig. 13d). A decrease in the content of starch *in vitro* plant tissues was due to the age of plant tissues. During *in vitro* conditions, a continuous increase in starch content with maximum accumulation occurs, which declines afterward till plantlets formation. This gradual increase in the starch content and explained that the accumulated starch was later used during plant organ formation and development. The upregulation of most genes related to starch and sucrose may be due to the fact that plants need to store carbohydrates to provide energy for stress defense (Thalmann et al. 2017).

3.5 Antioxidant Potential

Reactive oxygen species (ROS) generation in response to physiochemical fluctuations are common in plants, posing a threat due to potential oxidative damage (Wu et al. 2023). *In vitro* conditions, with reduced photosynthetic capacity and increased humidity, amplify ROS production. Both *in vivo* and *in vitro* plants employ non-enzymatic and enzymatic mechanisms to counteract ROS-induced damage.

3.5.1 Free Radical Scavenging Activity study via DPPH assay

DPPH (1, 1-Diphenyl-2-picrylhydrazyl radical) assay is a widely employed method for assessing the antioxidant potential of plants. The highest free radical scavenging activity (88.45 ± 0.081% and 86.29 ± 0.048%, respectively) was observed in shoot tip with cotyledon and hypocotyl cultures when cultures were treated with 8.0 mg/L of biogenic AgNPs and the activity was lowered down (78.85 ± 0.03% and 78.68 ± 0.04%, respectively) when the concentration of AgNPs was reduced to 2.0 mg/L. Field-grown leaves, shoots, and roots displayed scavenging activities of 82.25 ± 0.06%, 78.21 ± 0.23%, and 65.30 ± 0.10%, respectively. Regenerated shoots in the control and AgNPs, (8.0 mg/L) of shoot tip with cotyledon procure cultures had scavenging activities of 78.50 ± 0.30% and 88.38 ± 0.16%, respectively, while regenerated roots in the control and AgNPs, (8.0 mg/L), had 62.53 ± 0.26% and 71.28 ± 0.10% scavenging, respectively (Fig. 14a). Consistent with our findings, previous studies have demonstrated an increase in DPPH radical scavenging activity with higher

concentrations of green-synthesized AgNPs in various plant sources, including *Helicteres isora* roots (Bhakya et al. 2016), *Desmostachya bipinnata* leaves (Guntur et al. 2018), and *in-vitro* cultures of *Caralluma tuberculata* (Amir A. et al. 2019).

3.5.2 Total Phenolic Compounds

Phenolic compounds are plant secondary metabolites with antioxidant properties. AgNPs (8.0 mg/L treated cultures of shoot tip with cotyledon and hypocotyl exhibited the highest phenolic content (185.68 ± 0.09 mg/g DW GAE, 179.40 ± 0.20 mg/g DW GAE, respectively), while at 12 mg/L both the cultures had the lowest accumulation (145.24 ± 0.08 mg/g DW GAE, 135.34 ± 0.16 mg/g DW GAE). Plant parts of field grown plants displayed varying phenolic levels (leaves: 156.78 ± 0.518 mg/g DW GAE, shoots: 69.71 ± 0.207 mg/g DW GAE, roots: 55.91 ± 0.097 mg/g DW GAE). Control and AgNPs (8.0 mg/L) treated regenerated shoots (140.44 ± 0.115 mg/g GAE and 178.71 ± 0.203 mg/g GAE, respectively) while regenerated roots (49.86 ± 0.133 mg/g DW GAE and 62.593 ± 0.095 mg/g DW GAE, respectively) had good amount of phenolic content highlighting the impact of silver nanoparticle treatment on phenolic content in different plant tissues (Fig. 14b). Armin et al. (2011) observed that *Alhagi maurorum* seeds had 23.83 mg gallic acid equivalent/g phenolic content AgNPs-elicited hairy roots of *Cucumis anguria* cultures showed higher phenolic levels, with 6.0 mg/L AgNPs enhancing the content more than 15.0 mg/L (Sajad et al. 2023).

3.5.3 Total Flavonoids Content

Flavonoids, encompassing flavonols, flavanones, flavones, anthocyanidins, and catechins, are prevalent natural compounds in plants, known for their diverse pharmacological effects, such as anti-inflammatory, anti-allergic, antibacterial, antiviral, and antithrombotic activities. Baviera et al. (2023) explored the anti-oxidative properties of flavonoids. Silver nanoparticle (AgNPs, 8.0 mg/L) exhibited the highest flavonoid content (71.38 ± 0.09 mg/gQE, 68.01 ± 0.07 mg/gQE), whereas AgNPs at higher concentration (12.0 mg/L) had accumulated the lowest (47.32 ± 0.16 mg/gQE, 45.45 ± 0.06 mg/gQE) flavonoids in shoot tips with cotyledon and hypocotyl cultures, respectively, Various field plant tissues demonstrated distinct flavonoid levels in roots (20.30 ± 0.08 mg/gQE,) shoots (41.24 ± 0.06 mg/gQE,), and leaves, (51.65 ± 0.15 mg/gQE). Regenerated shoots exhibited 41.35 ± 0.06 mg/gQE and 55.41 ± 0.09 mg/gQE, while regenerated roots had 18.28 ± 0.10 mg/gQE and 28.30 ± 0.10 mg/gQE flavonoid content in control and treated (8.0mg/LAgNPs) materials, respectively (Fig. 14c). Sajad et al. (2023) observed enhanced flavonoid contents in wheat seedlings under *in-vitro* condition with 6.0 mg/L of *Alnus nitida* AgNPs and urea doped AgNPs, while 15.0 mg/L U-AgNPs resulted in lower flavonoids, suggesting an optimal concentration play important role. Additionally, Hasan et al. (2021) noted that 25.0 ppm and 50.0 ppm AgNPs on *Lactuca sativa* had positive effect, but 100.0 ppm AgNPs reduced the flavonoids.

3.6 Enzymatic Activity

3.6.1 Superoxide Dismutase (SOD) Activity

Superoxide Dismutase (SOD) is the primary ROS defense enzyme, converting superoxide radicals to H_2O_2 and mitigating oxidative damage. *In vitro*-derived tissues elevated SOD activity, as indicated by NBT inhibition. Silver nanoparticle (8.0 mg/L)-treated samples displayed the highest inhibition percentages 97.83 ± 1.48% for shoot tip with cotyledon culture and 93.34 ± 0.10% of hypocotyl culture while lower inhibition 78.007 ± 0.472% and 74.543 ± 0.138%, respectively from both the cultures were noticed at 2.0 mg/L of green AgNPs. A good inhibition percentage of SOD was observed in field-grown leaves (71.28 ± 0.161%), shoots (70.36 ± 1.03%), and roots (48.78 ± 3.28%). Regenerated shoots of control culture had 72.49 ± 0.16% inhibition, while AgNPs (8.0mg/L) treated shoots from shoot tip with cotyledon showed higher inhibition (81.54 ± 0.17%). Regenerated Roots of control had 58.34 ± 0.11%, and treatment (AgNPs, 8.0 mg/L) had 60.04 ± 2.80% inhibition activity (Fig. 14d). The impact of silver nanoparticles on superoxide dismutase activity depended on multiple parameters when evaluating AgNP-induced responses in plant antioxidant systems. Studies have demonstrated an increase (Morales et al. 2013; Nair et al. 2017; Amir Ali et al. 2019; Mubashir Hussain et al. 2017; Guntur et al. 2018), a decrease (Vardar et al. 2019; Cvjetko et al. 2017) of SOD activity.

3.6.2 Peroxidase (POD) Activity

Peroxidase enzyme effectively catalyzes the detoxification of H_2O_2 into less reactive oxygen species and water, measured as U (µmoles/min). Among the samples of shoot tip with cotyledon and hypocotyl cultures, silver nanoparticles (8.0mg/L) displayed the highest peroxidase activity at 2.54 ± 0.01 U and 2.42 ± 0.01 U, respectively. A higher concentration of AgNPs (12.0 mg/L) exhibited the lowest activity at 1.23 ± 0.01 U and 1.54 ± 0.01 U in both the cultures. Field-grown leaves, shoots, and roots had peroxidase activities of 1.54 ± 0.01 U, 1.452 ± 0.01 U, and 0.68 ± 0.01 U, respectively. Regenerated shoots and roots showed varying peroxidase activities under control and AgNPs treated cultures (Fig. 15a). Stable peroxidase activity in *in vitro* culture reflects changing plant interactions across growth regulators and developmental stages. This is consistent with findings in *Caralluma tuberculate*, where AgNPs treatment increased the peroxidase activity with the increasing concentration from control, 30.0 mg/L, and 60.0 m/L to 90.0 mg/L, i.e., 0.7, 1.9, 2.3 and 3.3 U/mg. protein,

respectively. (Amir et al. 2019). In a study conducted by Mehrian et al. (2015), the peroxidase activity in *Lycopersicon esculentum* shoots exhibited a significant increase at all the tested AgNPs concentrations (0.0, 25.0, 50.0, and 100.0 mg/L) compared to the control with activity values of 0.106 U, 0.169 U, 0.165 U, 0.217 U, and 0.193 U, respectively.

3.6.3 Catalase (CAT) Activity

Catalase is responsible for hydrogen peroxide decomposition into oxygen and water and it is quantified as U (μmoles H_2O_2/min). Notably, AgNPs (8.0 mg/L)-treated samples of shoot tip with cotyledon and hypocotyl cultures exhibited the highest catalase activity at 65.63 ± 0.29 U and 65.50 ± 0.3 U, while higher concentration of ANNPs (12.0mg/L) displayed lower activity at 47.52 ± 0.22 U and 43.38 ± 0.19 U in both the cultures. Field-grown leaves, shoots, and roots had catalase activities of 51.45 ± 0.12 U, 48.01 ± 0.15 U, and 38.29 ± 0.09 U, respectively. Regenerated shoots from shoot tip with cotyledon in the control and AgNPs treated samples showed catalase activities of 44.35 ± 0.12 U and 64.7 ± 0.091 U, respectively. In contrast, regenerated roots from shoot tip with cotyledon in the control and AgNPs treated samples displayed catalase activities of 37.38 ± 0.07 U and 45.62 ± 0.12 U, respectively (Fig. 15b). Our research is consistent with findings of Amir et al. (2019) in *Caralluma tuberculata*, where CAT levels rose after AgNPs treatment with 30.0 mg/L, 60.0 mg/L, and 90.0 mg/L of NPs to 0.8, 1.2, and 2.5 U/mg-protein, respectively. According to Mehrian et al. (2015), catalase activity increased significantly in shoots of *Lycopersicon esculentum* at all AgNPs concentrations at 0, 25.0, 50.0, 75.0 and 100.0 mg/L to 0.71, 1.15, 1.24, 1.55, and 1.17 U when compared with control. Notably, at the highest concentration of 100 .0 mg/L, catalase (CAT) activity declined.

3.6.4 Ascorbate Peroxidase (APX) Activity

In plants, the ascorbate-glutathione cycle is a vital system for hydrogen peroxide (H_2O_2) detoxification, where ascorbate peroxidase (APX) facilitates the conversion of H_2O_2 into water, utilizing ascorbate as an electron donor. AgNPs (8.0 mg/L) treated samples shoot tip with cotyledon and hypocotyl demonstrated the highest APX activity at 0.61 ± 0.02 mM/mg fresh weight and 0.49 ± 0.01 mM/mg fresh weight (FW), respectively, while lower activity exhibited at 0.26 ± 0.02 mM/mg FW and 0.2 ± 0.01 mM/mg FW in both the cultures at higher AgNPs (12.0 mg/L). Field-grown leaves, shoots, and roots displayed APX activities of 0.35 ± 0.003 mM/mg FW, 0.34 ± 0.004 mM/mg FW, and 0.21 ± 0.006 mM/mg FW, respectively. Regenerated shoots in the control and 8.0 mg/L AgNPs treatment groups exhibit APX activities of 0.326 ± 0.003 mM/mg FW and 0.487 ± 0.004 mM/mg FW, respectively. In contrast, regenerated roots in the control and 8.0 mg/L AgNPs treatment groups showed APX activities of 0.16 ± 0.002 mM/mg FW and 0.27 ± 0.003 mM/mg FW, respectively (Fig. 15c). Stable ascorbate peroxidase activity suggests potential variations in free radical generation or plant cell interactions across developmental stages, consistent with findings in *Caralluma tuberculate* (Amir et al. 2019). Homaee et al. (2012) found that ascorbate peroxidase activity was reduced at AgNPs treatment of 20.0 mg/L (0.6 U) on *Solanum tuberosum* maximum at 10.0 mg/L (0.11 U) AgNPs treatment.

3.6.5 Glutathione Reductase (GR) Activity

Glutathione reductase (GR) is a secondary defense enzyme against ROS. It regenerates the reduced glutathione (GSH) which is measured as U (mmol's DTNB/min). Among the samples, the highest GR activity was observed in shoot tip with cotyledon cultures (0.96 ± 0.006 U) and hypocotyl derived culture (0.78 ± 0.01 U) of 8.0 mg/L AgNPs treatments. At the same time, a higher amount of AgNPs (12.0mg/L) displayed the lowest GR activity at 0.57 ± 0.015 U and 0.47 ± 0.01 U in both the mentioned culture samples. Field-grown leaves, shoots, and roots have GR activities of 0.78 ± 0.003 U, 0.56 ± 0.002 U, and 0.29 ± 0.003 U, respectively. Regenerated shoots in the control and AgNPs treatment (8.0 mg/L) groups exhibited GR activities of 0.55 ± 0.01 U and 0.82 ± 0.003 U, respectively. In contrast, regenerated roots in the control and AgNPs treatment (8.0 mg/L) groups showed GR activities of 0.27 ± 0.004 U and 0.43 ± 0.01 U, respectively (Fig. 15d). In the present study, *Alhagi maurorum* plant parts and *in vitro*-materials showed a good antioxidant enzymatic activity. Homaee et al. (2012) observed that Glutathione Reductase activity was influenced by AgNPs treatment with nm size of NP with 2.0, 10.0, 20.0 mg/L concentrations in *Solanum tuberosum*. The activities of these enzymes (0.17 U and 0.20 U) were found maximum with 2.0 and 10.0 mg/L AgNPs treatment but declined at 20.0 mg/L (0.09 U) compared to the control.

3.7 High Performance Liuid Chromatography

HPLC analysis employed an Acetic Acid and Acetonitrile as mobile phase (0.1:99.9 ratio), achieving complete baseline separation of lupeol standard at a retention time of 4.25. Lupeol detection via HPLC analysis was performed using best-responding calli-derived roots (6 mg/L AgNPs) and control media roots, showing a retention time of 4.268 and 4.251, respectively, confirming lupeol presence specifically in the root samples (Fig. 16). At the same time, the shoots from the calli did not exhibit retention in that range.

Laghari et al. 2011, successfully detected Lupeol in the root bark of *Alhagi maurorum* with the retention time of 4.0 min. This was the first study to confirm the presence of Lupeol in plant tissue culture for this plant. Lupeol, found in *A. maurorum*, serves as a potential anticarcinogenic agent. It is a key component responsible for the plant's reported anticancer activity. Studies have shown its effectiveness

in inhibiting tumor promotion in skin carcinogenesis, with topical application reducing tumor burden multiplicity and increasing tumor latency period in mice. It also suppresses early tumor growth induced by benzoyl peroxide. The abundant presence of lupeol in the plant suggests its future use as a source for pharmaceutical formulations. Many studies highlighted its multi-target mechanism of action, with no observed toxicity to normal cells and tissues at therapeutic doses (Saleem, 2009; Laghari et al. 2015).

Conclusion

Alhagi maurorum, a valuable medicinal plant, addressed the imperative need for sustainable strategies to elevate biomass production and amplify the yield of therapeutic compounds. The research achieved a pivotal milestone by successfully standardizing a protocol for conservation and sustainable biomass production of this valuable medicinal plant. Notably, the incorporation of biogenic silver nanoparticles (AgNPs) *in vitro*, in conjunction with plant growth regulators and other adjuvants resulted in remarkable callus proliferation and differentiation, demonstrating the potential of nanotechnology in plant tissue culture. The intriguing discovery that AgNPs, when applied independently, induced a substantial increase in the biosynthesis of diverse antioxidant secondary metabolites opens new avenues for medicinal applications.

However, the journey towards unlocking the full potential of green-synthesized AgNPs (ranging from 7 to 30 nm) with 2.0-8.0 mg L^{-1} concentrations exhibited significant growth enhancement and antioxidant enzyme production but higher concentrations showed inhibitory effects. As we advance in this field, further research is essential to unveil the intricate molecular mechanisms underlying the impact of nanoparticles on cell development and secondary metabolism. Additionally, understanding the movement and chemistry of nanoparticles remains pivotal in addressing future health challenges posed by *Alhagi maurorum* and similar plants. In summary, this study establishes a foundation for sustainable plant bioprocessing and highlights the promising role of AgNPs in enhancing plant growth and medicinal metabolite production. The journey towards harnessing the full potential of nanotechnology in medicinal plants continues, propelled by the pursuit of more profound insights into the intricate interactions between nanoparticles and plant biology.

Declarations

Author Contributions

D.B., A.R.S. and A.S. to the conception and design of the study. D.B. and A.S. performed the statistical analysis and data interpretation. D.B. and A.S. wrote the first draft of the manuscript. A.S. and N. Supported the lab work experiments. A.R.S. for editing and overall support of the study. All authors have read and agreed to the published version of the manuscript.

Funding

This research received no specific grant from any public, commercial, or not-for-profit funding agency.

Competing interests

The authors have no relevant financial or non-financial interests to disclose.

Data availability

Data sharing is not applicable to this article as no datasets were generated.

References

1. Aebi H (1984) Catalase in vitro. Methods Enzymol. 105:121-6. doi:10.1016/s0076-6879(84)05016-3.
2. Agarwal T, Gupta AK, Patel AK, Shekhawat NS (2015) Micropropagation and validation of genetic homogeneity of *Alhagi maurorum* using SCoT, ISSR and RAPD markers Plant Cell Tiss Organ Cult, 120:313–323 doi.org/10.1007/s11240-014-0608-z
3. Aghdaei M, Salehi H, Sarmast MK (2012) Effects of silver nanoparticles on Tecomella undulata (Roxh.) Seem. micropropagation. Adv. Hortic. Sci, 26, 21–24. https://doi.org/10.13128/ahs-12748

4. Ahmad S, Ahmad I, Saleem M (2009) Secondary metabolites from *Alhagi maurorum*. *J Chem Soc Pak*. **31** (6): 960–963. https://www.researchgate.net/publication/288131442_Secondary_metabolites_from_Alhagi_maurorum
5. Ahmad M, Khan MA, Marwat SK (2009) Useful medicinal flora enlisted in Holy Quran and Ahdith. Am Eurasian. J Agric Environ Sci, 5(1):126-140. https://www.researchgate.net/publication/326690189_Useful_Medicinal_Flora_Enlisted_in_Holy_Quran_and_Ahadith
6. Amer A (2019) Biotechnology approaches for in vitro production of flavonoids. J. Microbiol. Biotechnol. Food Sci. 2019, 457–468. http://dx.doi.org/10.15414/jmbfs.2018.7.5.457-468
7. Amir A, Mohammad S, Khan MA, Raja NI, Arif M, Kamil A, Mashwani ZR (2019) Silver Nanoparticles Elicited in Vitro Callus Cultures for Accumulation of Biomass and Secondary Metabolites in Caralluma tuberculata. Artif. Cells Nanomed. Biotechnol, 47, 715–724. https://doi.org/10.1080/21691401.2019.1577884
8. Armin O, Oskoueian, E, Hendra R, Farida Z, Samadi F, Karimi E (2011) Antioxidant activity and bioactive compounds in *Alhagi maurorum*. Clin Biochem. 44. S343-S344 % @ 0009. 10.1016/j.clinbiochem.2011.08.856
9. Asada K (1992) Ascorbate peroxidase-a hydrogen peroxidescavenging enzyme in plants. Physiol Plant 85: 235-241 https://doi.org/10.1111/j.1399-3054.1992.tb04728.x
10. Azooz MM, Elhamd MFA, Al-Fredan MA (2012) Biphasic effect of copper on growth, proline, lipid peroxidation and antioxidant enzyme activities of wheat (Triticum aestivum cv. Hasaawi) at early growing stage. Austr J of Crop Sci, 6, 688–694.
11. Bahamin N, Ahmadian S, Rafieian-Kopaei M, Mobini G, Shafiezadeh M, Soltani AA (2021) Comparative Study on Anticancer Effects of the *Alhagi maurorum* and *Amygdalus haussknechtii* Extracts Alone and in Combination with Docetaxel on 4T1 Breast Cancer Cells. Evid Based Complem Alternat Med. Jun 14, 2021:5517944. https://doi.org/10.1155/2021/5517944
12. Bamal D, Singh A, Chaudhary G, Kumar M, Singh M, Rani N, Mundlia P, Sehrawat AR (2021) Silver Nanoparticles Biosynthesis, Characterization, Antimicrobial Activities, Applications, Cytotoxicity and Safety Issues: An Updated Review. Nanomaterials, 11, 2086. https://doi.org/10.3390/nano11082086
13. Baviera R D, Ruiz-Canales A, Barrajon-Catalan E. *Cistus albidus* L (2023) Review of a Traditional Mediterranean Medicinal Plant with Pharmacological Potential. Plants, 12, 2988. https://doi.org/10.3390/plants12162988
14. Bhakya S, Muthukrishnan S, Sukumaran M (2016) Biogenic synthesis of silver nanoparticles and their antioxidant and antibacterial activity. Appl Nanosci 6, 755–766 https://doi.org/10.1007/s13204-015-0473-z
15. Blois MS (1958) Antioxidant determination by the use of a stable free radical. Nature, 461 7, 1198-1200. http://dx.doi.org/10.1038/1811199a0
16. Bradford MM (1976) A rapid and sensitive for the quantitation of microgram quantitites of protein utilizing the principle of protein-dye binding. Analy Biochem 72: 248-254. https://doi.org/10.1006/abio.1976.9999
17. Bruna T, Maldonado-Bravo F, Jara P, Caro N (2021) Silver Nanoparticles and Their Antibacterial Applications. Int J Mol Sci. Jul 4,22 (13):7202. doi: 10.3390/ijms22137202
18. Cao G, Wang Y (2011) Nanostructures and Nanomaterials, World Scientific Series in Nanoscience and Nanotechnology, World Scientific: Singapore, Volume 2, ISBN 978-981-4322-50-8.
19. Chance B, Maehly AC (1955) Assay of catalase and peroxidase. Methods Enzymol 2:764, 775. http://dx.doi.org/10.1016/S0076-6879(55)02300-8
20. Chapman HN, Fromme P, Barty A, White TA, Kirian R, Aquila A, Hunter MS, Schulz J, DePonte DP, Weierstall U (2011) Femtosecond X-ray protein nanocrystallography. Nat. Cell Biol, 470, 73–77. doi: 10.1038/nature09750
21. Chen L, Qi C, Zhengzhu Z, Xiaochun W (2009) A novel colorimetric determination of free amino acids content in tea infusions with 2,4-dinitrofluorobenzene. J of Food Comp and Anal 22 137–141 http://dx.doi.org/10.1016/j.jfca.2008.08.007
22. Cvjetko P (2017) Toxicity of silver ions and differently coated silver nanoparticles in *Allium cepa* roots. *Ecotoxicol. Environ. Saf*. **137**, 18–28. https://doi.org/10.1016/j.ecoenv.2016.11.009
23. Devi JS, Bhimba BV, Peter DM (2013) Production of biogenic silver nanoparticles using *Sargassum longifolium* and its applications. Indian J. Geo-Marine Sci. 42 (1), 125–130.
24. Dubois M, Gilles KA, Hamilton JK, Rebers PA, Smith F (1956) Colorimetric method for determination of sugars and related substances. Anal. Chem. 28:350-356. https://doi.org/10.1021/ac60111a017
25. Guntur SR, Kumar NS, Hegde MM, Dirisala VR (2018) In vitro studies of the antimicrobial and free-radical scavenging potentials of silver nanoparticles biosynthesized from the extract of *desmostachya bipinnata*. Anal. Chem. Insights 13, 1. doi:10.1177/1177390118782877

26. Haida Z, Hakiman M (2019) A comprehensive review on the determination of enzymatic assay and nonenzymatic antioxidant activities. Food sci & nutri, 7(5), 1555-1563. https://doi.org/10.1002%2Ffsn3.1012
27. Hansen and Moller (1975) Percolation of Starch and Soluble Carbohydrates from Plant Tissue for Quantitative Determination with Anthrone. Analy Biochem 68, 87-94. https://doi.org/10.1016/0003-2697(75)90682-x
28. Hasan M, Mehmood K, Mustafa G, Zafar A, Tariq T, Hassan S G, Loomba S, Zia M, Mazher A, Mahmood N, Shu X (2021) Phytotoxic evaluation of phytosynthesized silver nanoparticles on lettuce, Coatings 11 1–15. https://doi.org/10.3390/coatings11020225
29. Hassanein AM and Mazen AMA (2001) Adventitious bud formation in *Alhagi graecorum.* Plant Cell Tiss Org.Cult **65** : 31 – 35. https://doi.org/10.1023/A:1010637407780
30. Homaee BM, Ehsanpour AA (2016) Silver nanoparticles and silver ions: Oxidative stress responses and toxicity in potato (*Solanum tuberosum* L) grown *in vitro.* Hortic. Environ. Biotechnol. 57, 544–553. https://doi.org/10.1007/s13580-016-0083-z
31. Hussain M (2017) In vitro germination and biochemical profiling of Citrus reticulata in response to green synthesised zinc and copper nanoparticles. IET Nanobiotechnol. 11(7), 790–796. https://doi.org/10.1049%2Fiet-nbt.2016.0256
32. Kainat S, Gilani SR, Asad F (2022) Determination and comparison of phytochemicals, phenolics, and flavonoids in Solanum lycopersicum using FTIR spectroscopy. Food Anal Methods 15:2931–2939. http://dx.doi.org/10.1007/s12161-022-02344-w
33. Khalid S, Arshad M, Mahmood S (2023) Extraction and Quantification of Moringa oleifera Leaf Powder Extracts by HPLC and FTIR. Food Anal. Methods 16, 787–797. https://doi.org/10.1007/s12161-023-02470-z
34. Khalifa HA, Shalaby SI, Abdelaziz AS (2019) Alhagi maurorum aqueous extract protects against norfloxacin-induced hepato-nephrotoxicity in rats. Chin Herb Med. 28;12(2):156-162. doi: 10.1016/j.chmed.2019.09.007
35. King LJ (1974) Weeds of the World: Biology and Control. Wiley Eastern Private Limited, New Delhi, 526 pp.
36. Kulieva AK, Shasvarov GDV (1972) (Article in Russian), 961.
37. Laghari A, Memon S, Nelofar A, Khan K (2011) *Alhagi maurorum*: A convenient source of lupeol. Industrial Crops and Products - IND CROP PROD. 34. 1141-1145. 10.1016/j.indcrop.2011.03.031
38. Liaqat N, Jahan N, Khalil UR, Anwar T, Qureshi H (2022) Green synthesized silver nanoparticles: Optimization, characterization, antimicrobial activity, and cytotoxicity study by hemolysis assay. Front Chem. 10:952006. doi: 10.3389/fchem.2022.952006
39. Liu X (2005) Effects of nano-ferric oxide on the growth and nutrients absorption of peanut. Plant Nutr. Fert. Sci **11**, 14–18.
40. Malabadi RB, Meti NT, Mulgund GS, Nataraja K, Vijaya SK (2012) Synthesis of silver nanoparticles from *in vitro* derived plants and callus cultures of *Costusspeciosus* (Koen.) assessment of antibacterial activity. Research in Plant Biology. **2** (4): 32 - 42.
41. McDonald S, Prenzler PD, Antolovich M, Robards K (2001) Phenolic content and antioxidant activity of olive extracts. Food Chem, 73, 73–84. https://doi.org/10.1016/S0308-8146(00)00288-0
42. Mehrian K, Saeed H, Reza R, Fatima (2015) Effect of silver nanoparticles on free amino acids content and antioxidant defense system of tomato plants. Ind J of Plant Physio. 20. DOI 10.1007/s40502-015-0171-6.
43. Misra HP and Fridovich I (1972). J. Biol. Chem, 247, 3130-3175 https://pubmed.ncbi.nlm.nih.gov/4623845/
44. Morales MI (2013) Toxicity assessment of cerium oxide nanoparticles in cilantro (*Coriandrum sativum* L.) plants grown in organic soil. J. Agric. Food Chem. **61**, 6224–6230. https://doi.org/10.1021/jf401628v
45. Murashige T, Skoog F (1962) A revised medium for rapid growth and bioassays with tobacco tissue cultures. Physiol Plant 15:473–497 https://doi.org/10.1111/j.1399-3054.1962.tb08052.x
46. Nair PMG and Chung IM (2014) Physiological and molecular level effects of silver nanoparticles exposure in rice (*Oryza sativa* L.) seedlings. Chemosphere **112**, 105–113. https://doi.org/10.1016/j.chemosphere.2014.03.056
47. Rajeshkumar S, Bharath LV (2017) Mechanism of plant-mediated synthesis of silver nanoparticles—A review on biomolecules involved, characterisation and antibacterial activity. Chem. Biol. Interact. 273, 219–227. https://doi.org/10.1016/j.cbi.2017.06.019
48. Sadasivam S and Manickam A (1990) Biochemical methods, new age International (P) Ltd.: New Delhi, India, pp.110–112.
49. Sadasivam S, Manickam A (1992) Biochemical methods for agricultural sciences. 12-13.
50. Sajad K, Raham SK, Muhammad Z, Sikandar K, Noor U I, Khan T, Zar M, Riaz U, Ahmed B (2023) *Alnus nitida* and urea-doped Alnus nitida-based silver nanoparticles synthesis, characterization, their effects on the biomass and elicitation of secondary metabolites in wheat seeds under in vitro conditions. Heliyon 9 e14579 https://doi.org/10.1016/j.heliyon.2023.e14579
51. Salama, HM (2012) Effects of silver nanoparticles in some crop plants, common bean (*Phaseolus vulgaris* L.) and corn (*Zea mays* L.). Int. Res. J. Biotechnol. **3**, 190–197.
52. Samal J (2016) Medicinal plants and related developments in India: a peep into 5-year plans of India. Ind. J Health Sci 9:14–19 http://dx.doi.org/10.4103/2349-5006.183698

53. Sehrawat AR and Malik A, Sehrawat K, Singh A, Bamal D (2021) Antimicrobial and in vitro Efficacy of Green Silver Nanoparticles in Tissue Culture of Alhagi maurorum. Nelumbo. 63. 243. https://doi.org/10.20324/nelumbo/v63/2021/165155
54. Shaikhaldein HO, Al-Qurainy F, Nadeem M, Khan S, Tarroum M, Salih AM (2020) Biosynthesis and characterization of silver nanoparticles using Ochradenus arabicus and their physiological effect on *Maerua oblongifolia* raised in vitro. Sci. Rep. 10 1–8, https://doi.org/10.1038/s41598-020-74675-9
55. Sharma P, Bhatt D, Zaidi MG, Saradhi PP, Khanna PK, Arora S (2012) Silver nanoparticlemediated enhancement in growth and antioxidant status of Brassica juncea. Appl Biochem Biotechnol 167:2225–2233 https://doi.org/10.1007/s12010-012-9759-8
56. Singleton VL and Joseph AR (1965) Colorimetry of Total Phenolics with Phosphomolybdic-Phosphotungstic Acid Reagents. Am J Enol Vitic. 16: 144-158. https://doi.org/10.5344/ajev.1965.16.3.144
57. Smith IK, Thomas LV, Carol AT (1988) Assay of Glutathione Reductase in Crude Tissue Homogenates Using 5,5'-Dithiobis(2-nitrobenzoic Acid). Anal Biochem 175.408-4 13 https://doi.org/10.1016/0003-2697(88)90564-7
58. Thalmann M and Santelia D (2017) Starch as a determinant of plant fitness under abiotic stress. New Phytologist, *214*(3), 943-951. https://doi.org/10.1111/nph.14491
59. Ubgade S, Bapat A, Kilor V (2021) Effect of various stabilizers on the stability of lansoprazole nanosuspension prepared using high shear homogenization: Preliminary investigation. J Appl Pharm Sci, 11(09):085–092 http://dx.doi.org/10.7324/JAPS.2021.110910
60. Vaou N, Stavropoulou E, Voidarou C, Tsigalou C, Bezirtzoglou E (2021) Towards Advances in Medicinal Plant Antimicrobial Activity: A Review Study on Challenges and Future Perspectives. Microorganisms. 27;9 (10):2041. doi: 10.3390/microorganisms9102041
61. Yanık F and Vardar F (2019) Assessment of silver nanoparticle-induced morphological, biochemical and physiological alterations in wheat roots. Ann. Bot. 9, 83–94. https://doi.org/10.13133/2239-3129/14633
62. Wu C, Mao J, Wang X (2023) Advances in treatment strategies based on scavenging reactive oxygen species of nanoparticles for atherosclerosis. J Nanobiotechnol 21, 271. https://doi.org/10.1186/s12951-023-02058-z
63. Zia M, Yaqoob K, Mannan A, Nisa S, Raza G, Rehman R (2020) Regeneration response of carnation cultivars in response of silver nanoparticles under in vitro conditions, Vegetos 33 11–20. http://dx.doi.org/10.1007/s42535-019-00074-9

Figures

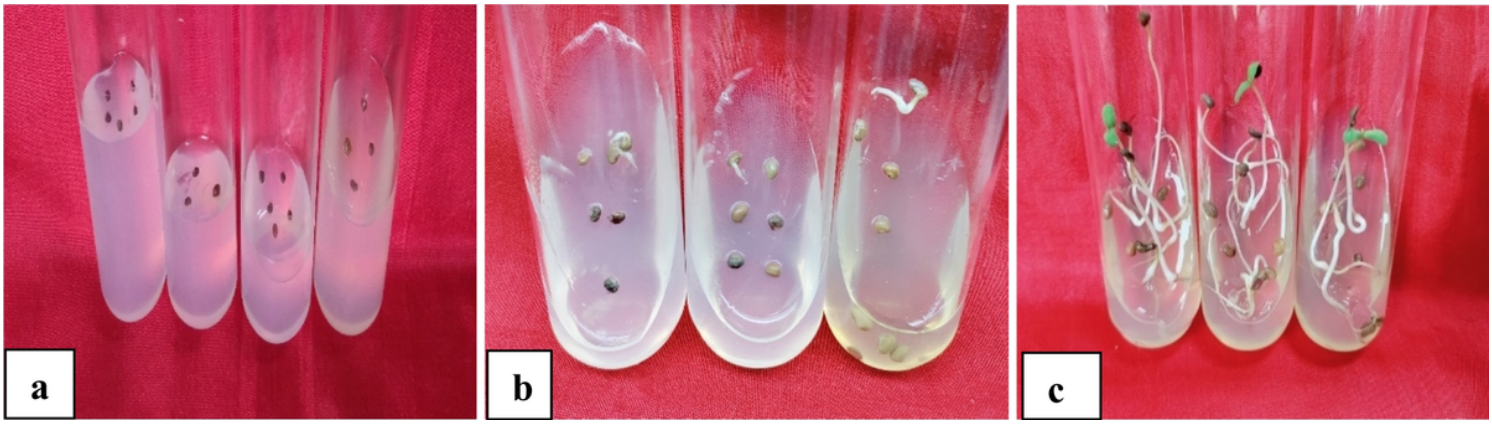

Figure 1

Seeds of *Alhagi Maurorum* inoculated on (a) Germination medium, (b) Seeds showing poor germination, (c) 10 days old seedling showing good germination

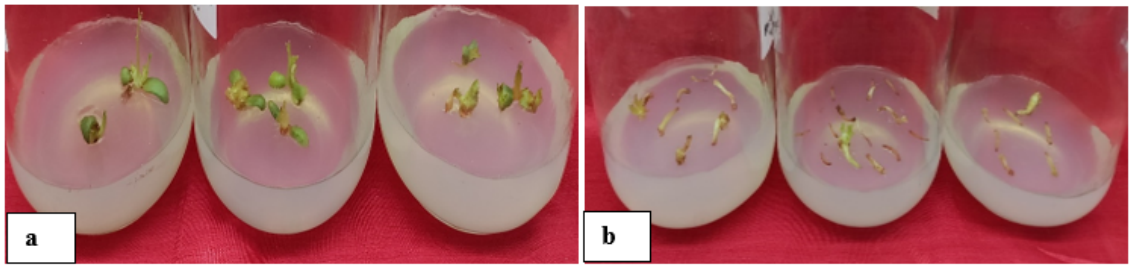

Figure 2

Culturing of (a) Shoot tip with cotyledon (C) and (b) hypocotyl (H) of 10 day old seedlings on MS medium

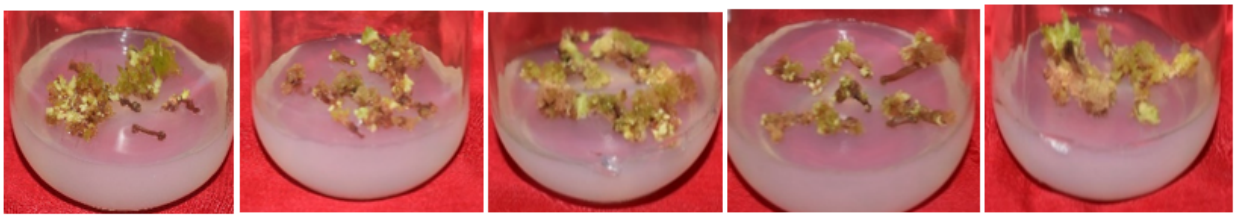

Figure 3

Callus growth from hypocotyl on MS medium after four weeks of culturing

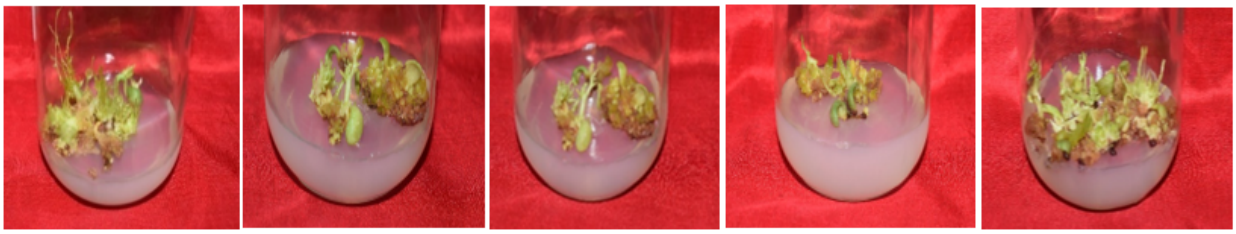

Figure 4

Callus growth from shoot tip with cotyledon on MS medium after four weeks of culturing

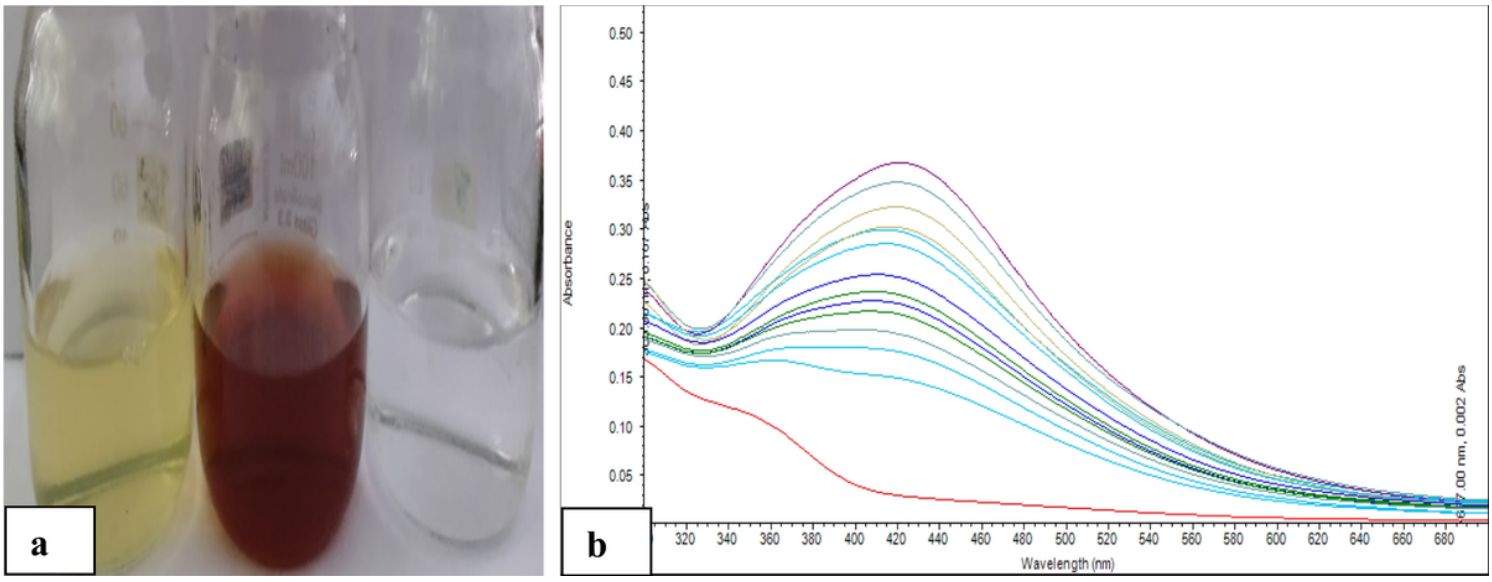

Figure 5

Fig. 6 (a) Biosynthesized silver nanoparticle (b) Stability of nanoparticles up to 60th day

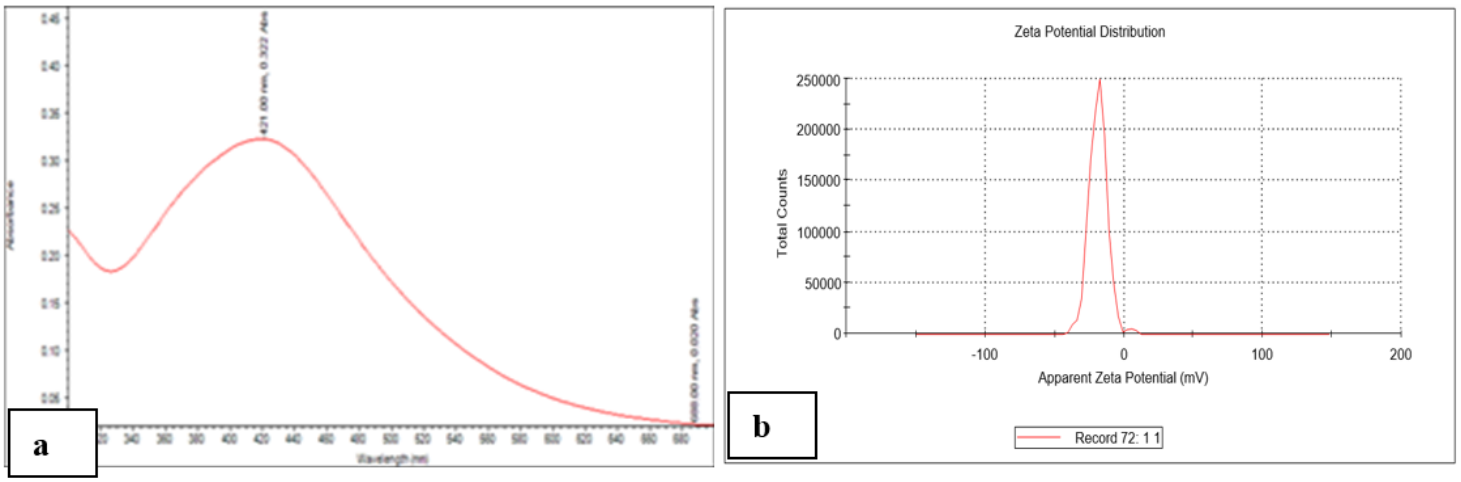

Figure 6

Fig. 7(a) UV-Vis absorption maxima at 419 nm (b) Zeta potential of Biosynthesized AgNPs

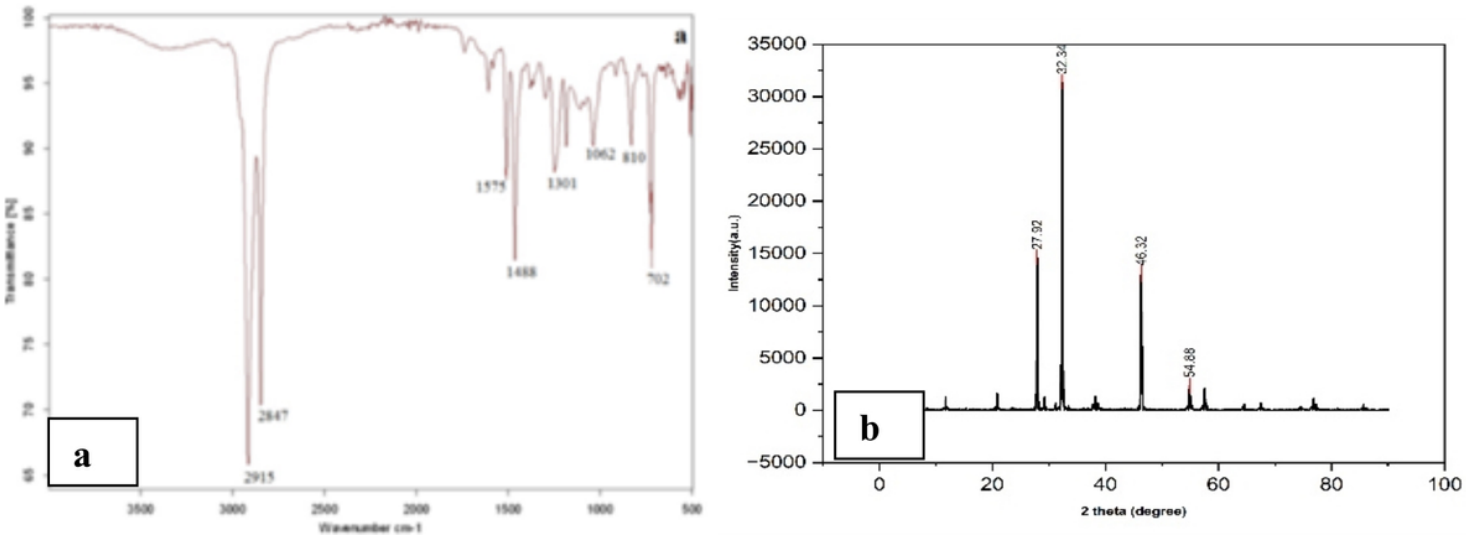

Figure 7

Fig. 8(a) FTIR image (b) XRD image powdered sample of AgNPs

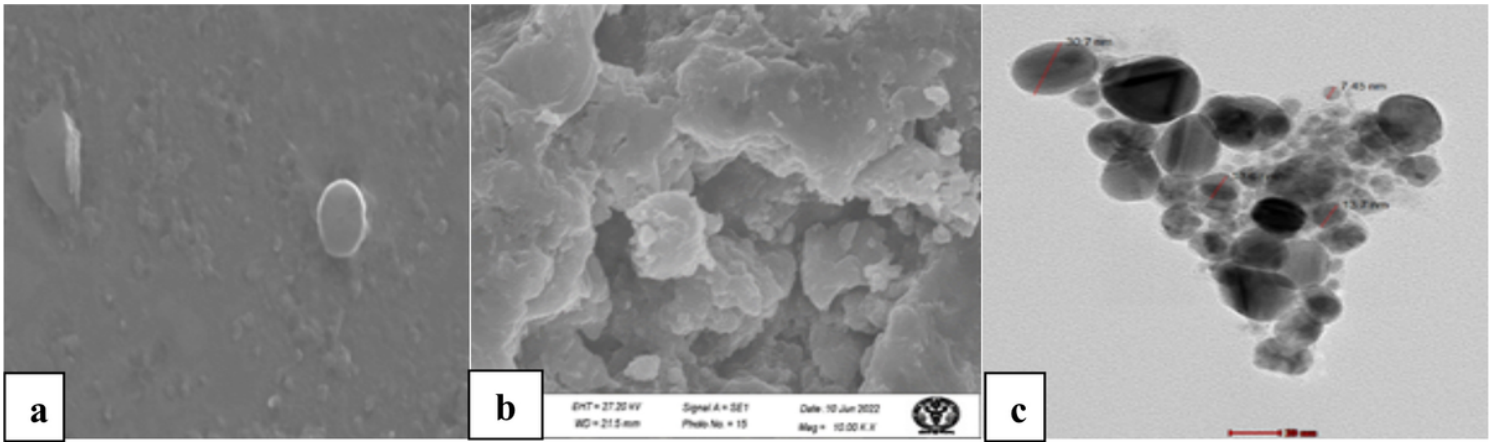

Figure 8

Fig. 9 SEM image (a) of liquid (b) Powdered sample (c) TEM image of AgNPs

Figure 9

Fig. 10 Growth of calli on the 90th day of sub-culturing from hypocotyl on control and treatment medium having AgNPs (2.0, 4.0, 6.0, 8.0, 10.0, and 12.0 mg/L).

Figure 10

Fig. 11 Growth of calli on the 90th day of sub-culturing from cotyledons with shoot tip on control and treatment medium having AgNPs (2.0, 4.0, 6.0, 8.0, 10.0, and 12.0 mg/L).

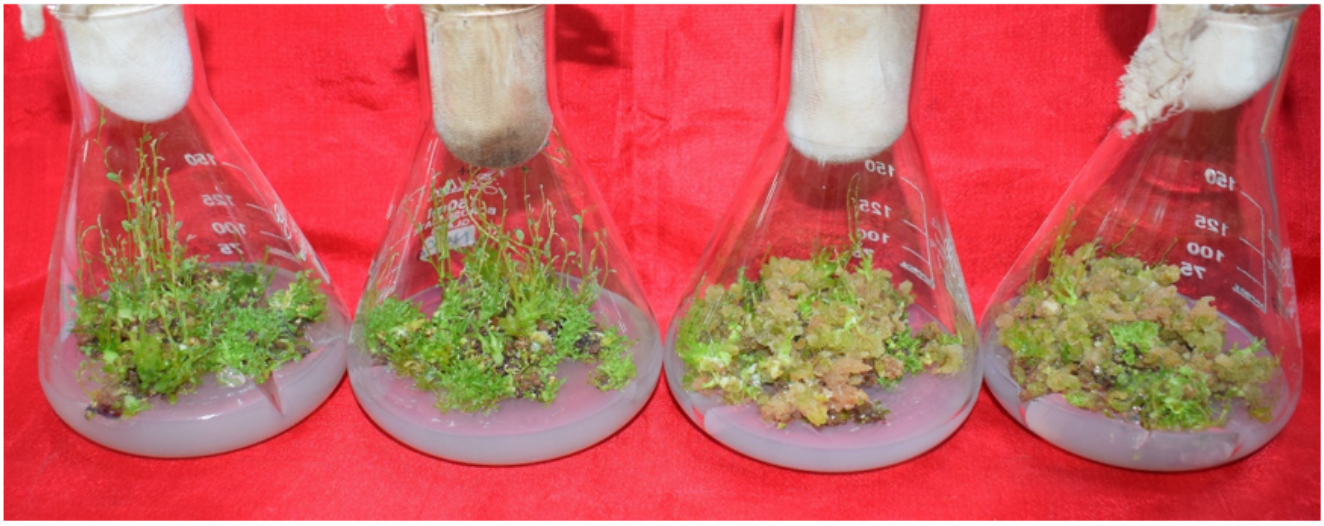

Figure 11

Fig. 12 Comparison of growth after sub-culturing of calli from cotyledons with shoot tip and hypocotyl medium having AgNPs, 4.0, 6.0 mg/L.

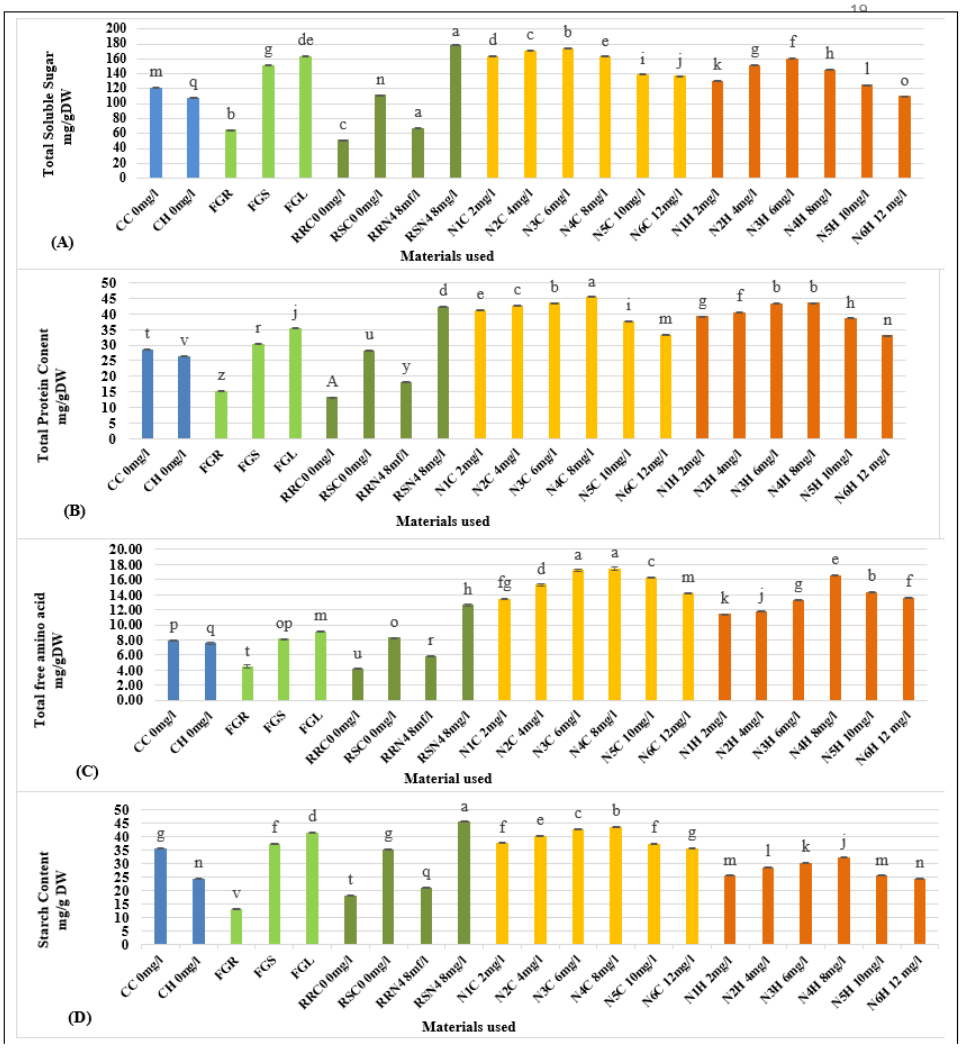

Figure 12

Fig. 13 Evaluation of (A) Total soluble sugar (B) Total Protein Content (C) Total Free Amino Acid (D) Total Starch Content in *in vitro* raised cultures and field-grown plant parts of *Alhagi maurorum* in control and different concentrations of biogenic AgNPs.. Data represents the mean values of triplicates with ± standard error. Column data with different letter/s differ significantly at $p<0.05$

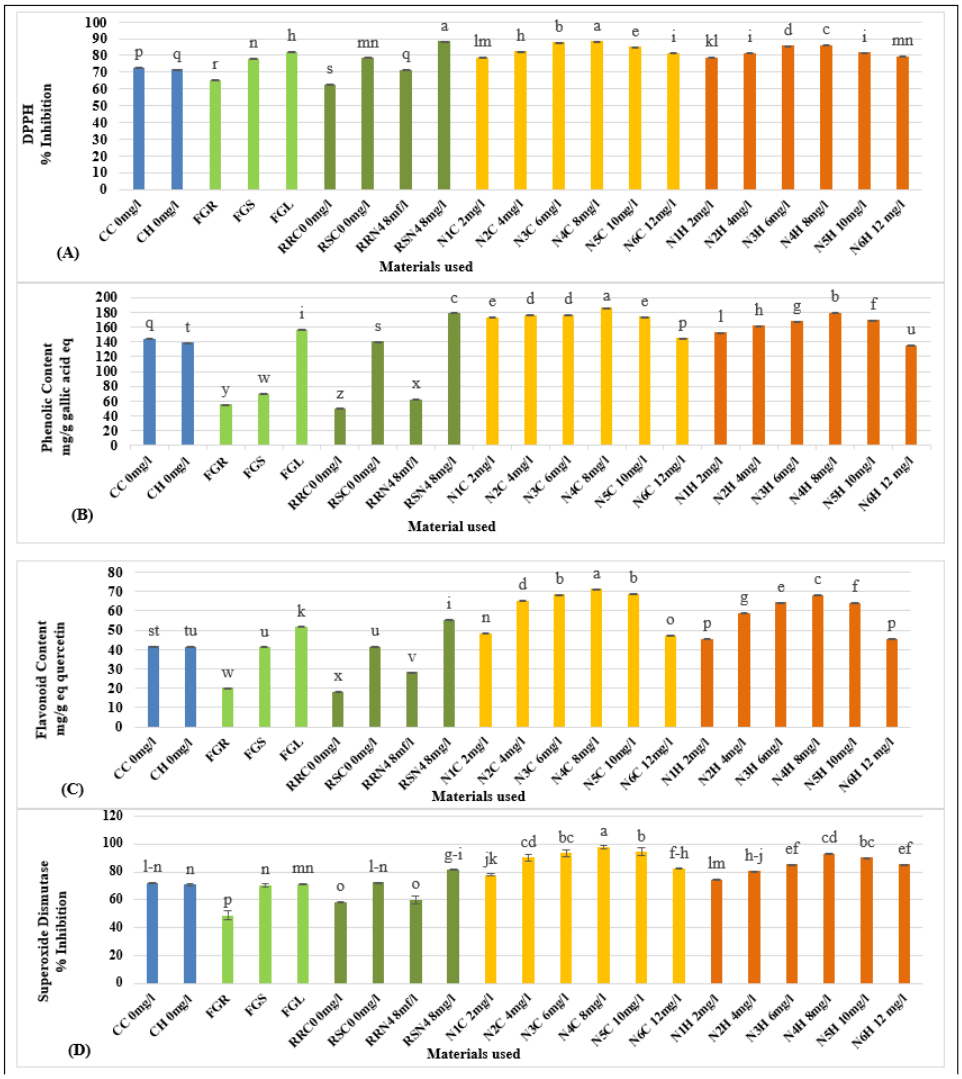

Figure 13

Fig. 14 Estimation of (A) Free radical scavenging activity via DPPH assay (B) Phenolic content (C) Flavonoids (D) Superoxide Dismutas in *in vitro* raised cultures and field-grown plant parts of *Alhagi maurorum* in control and different concentrations of biogenic AgNPs. . Data represents the mean values of triplicates with ± standard error. Column data with different letter/s differ significantly at $p<0.05$

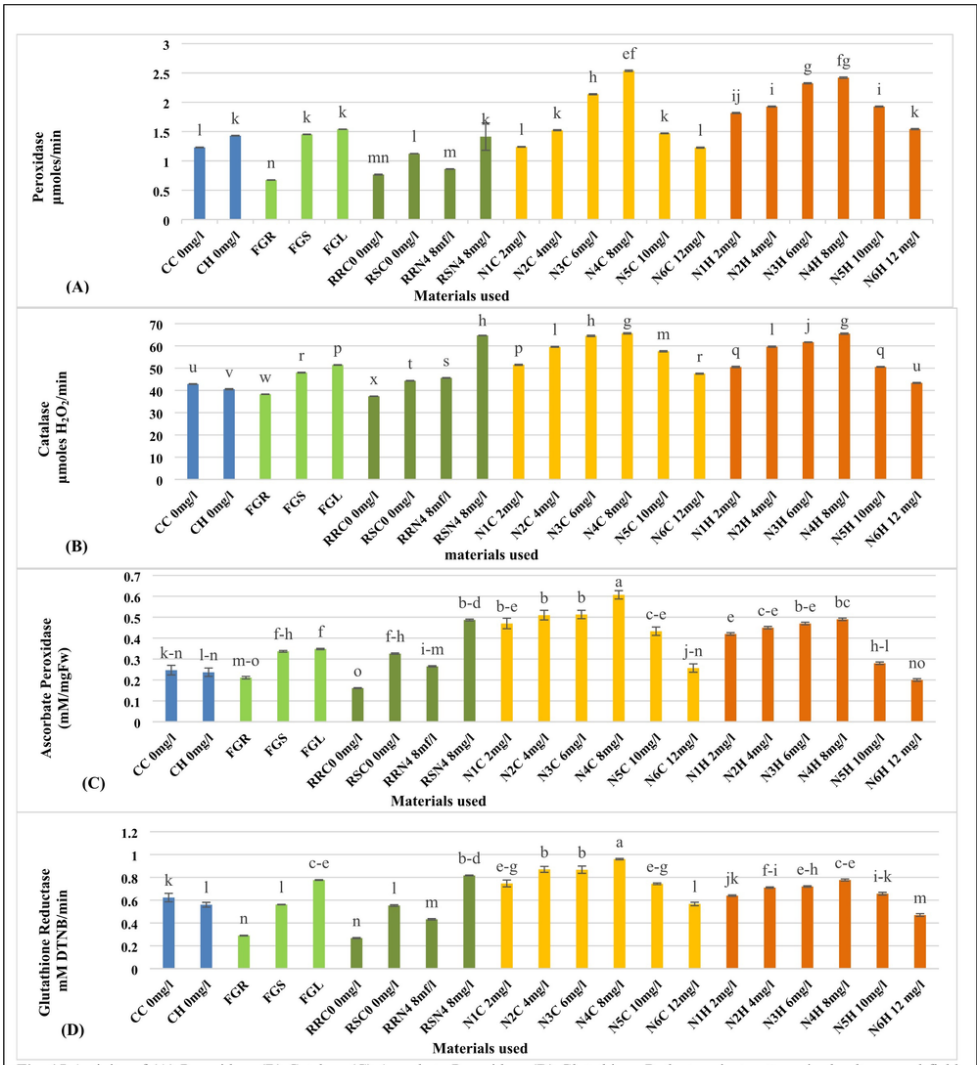

Fig. 15 Activity of (A) Peroxidase (B) Catalase (C) Ascorbate Peroxidase (D) Glutathione Reductase in *in vitro* raised cultures and field-grown plant parts of *Alhagi maurorum* in control and different concentrations of biogenic AgNPs. Data represents the mean values of triplicates with ± standard error. Column data with different letter/s differ significantly at $p<0.05$

Figure 14

See image above for figure legend

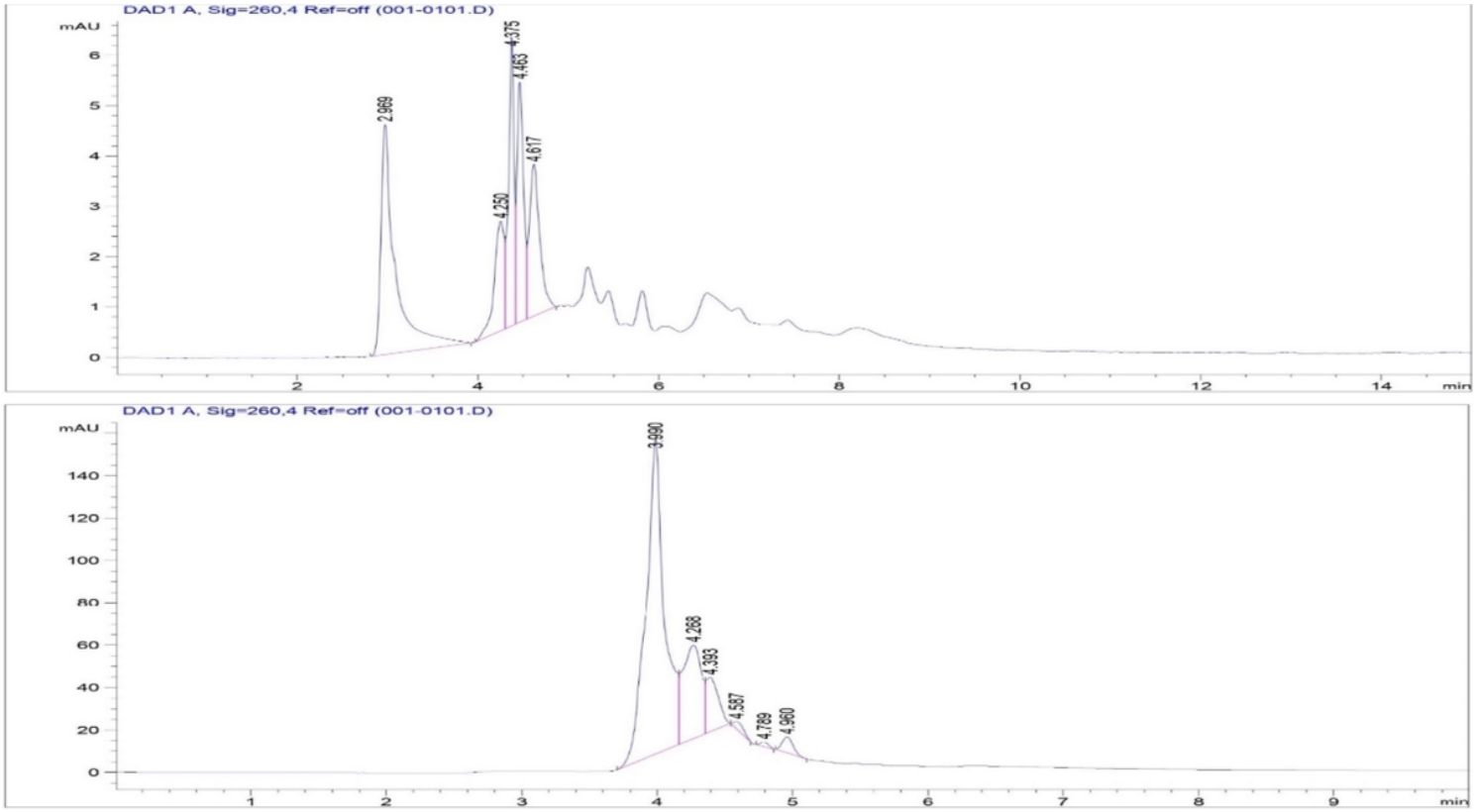

Figure 15

Fig. 16 High Performance Liquid Chromatography profile of (a) Lupeol and (b) Regenerated roots of *Alhagi mauraorm*